Available online at www.sciencedirect.com

SCIENCE DIRECT

Biochimica et Biophysica Acta 1711 (2005) 72–86

BIOCHIMICA ET BIOPHYSICA ACTA BBA

http://www.elsevier.com/locate/bba

Electrostatic basis of valence selectivity in cationic channels

Ben Corry[a,*], Taira Vora[b], Shin-Ho Chung[b]

[a]Chemistry, School of Biomedical and Chemical Sciences, The University of Western Australia, Crawley, WA, 6009, Australia
[b]Department of Theoretical Physics, Research School of Physical Sciences, The Australian National University, Canberra, 0200, Australia

Received 17 January 2005; received in revised form 3 March 2005; accepted 4 March 2005
Available online 24 March 2005

Abstract

We examine how a variety of cationic channels discriminate between ions of differing charge. We construct models of the KcsA potassium channel, voltage gated sodium channel and L-type calcium channel, and show that they all conduct monovalent cations, but that only the calcium channel conducts divalent cations. In the KcsA and sodium channels divalent ions block the channel and prevent any further conduction. We demonstrate that in each case, this discrimination and some of the more complex conductance properties of the channels is a consequence of the electrostatic interaction of the ions with the charges in the channel protein. The KcsA and sodium channels bind divalent ions strongly enough that they cannot be displaced by other ions and thereby block the channel. On the other hand, the calcium channel binds them less strongly such that they can be destabilized by the repulsion of another incoming divalent ion, but not by the lesser repulsion from monovalent ions.

Keywords: Ion channel; Selectivity; Sodium channel; Calcium channel; Potassium channel; Brownian dynamics; Block; Electrostatics

1. Introduction

Most ion channels demonstrate a high degree of selectivity for one type of ion over others, and yet in many cases, how they manage to achieve this is still not clear. It is generally accepted that the distribution of charges in ion channel proteins is responsible for their selectivity for either cations or anions. In the KcsA potassium channel, for example, carbonyl oxygen atoms point into the narrow selectivity filter section of the pore. The negative partial charges carried by these atoms attracts cations into the channel, while repelling anions. Indeed, a monovalent cation sees a deep energy well in this region of about 67 kT [1] while a monovalent anion sees an energy barrier of a similar magnitude. In the gramicidin pore, although the protein has a net neutral charge, the presence of more negative partial charges near the pore makes the channel selective to cations [2]. In selective channels, the orientation of polar residues, or the presence of charged ionizable residues, yields a distribution of charges that attracts ions of one charge while repelling those of the opposite sign.

An issue that has been less well discussed is how channels select between ions with the same sign but different magnitude of charge. For example, why does a channel favor divalent ions over monovalent ions, and why does one type conduct while the other does not? The calcium channel, for example, conducts monovalent ions when no divalent ions are present in the surrounding solution, but the channel allows only divalent ions to pass as soon as they are present [3]. In other cation channels, such as the families of potassium and sodium channels, monovalent ions conduct readily, but divalent ions do not. Indeed, the presence of divalent ions can stop conduction all together (see [4] and references therein; [5]). Given that the charge distribution in the channel creates the selectivity between cations and anions, it is not surprising that these channels respond differently to monovalent and divalent ions.

While there is a strong case that the selectivity for either divalent or monovalent ions arises directly from the electrostatic interaction with the partial charges in the channel walls [6–9], there are still some alternative theories

* Corresponding author. Fax: +61 8 6488 1005.
E-mail address: ben@theochem.uwa.edu.au (B. Corry).

0005-2736/$ - see front matter © 2005 Elsevier B.V. All rights reserved.
doi:10.1016/j.bbamem.2005.03.002

in which both electrostatics and volume are important. Nonner et al. [10] and Boda et al. [11] both proposed a model in which valence selectivity arises from competition between charge and available space. They hypothesise that the selectivity filter of the calcium channel is a finite space in which the negatively charged oxygens from the surrounding glutamate residues are confined. Calcium ions are preferred to sodium in this model as they have the same charge neutralising effect as two sodium ions, while occupying less of the limited volume in the filter. As we will discuss below, we believe that electrostatic properties alone (i.e. without considering limited volume) are enough to explain monovalent or divalent ion selectivity. A further discussion of the difference between our model and these theories is presented in the Concluding Remarks section.

More recently, applied field non-equilibrium molecular dynamics studies of the calcium channel have been conducted based on either the charge-space competition model [12] or with the glutamate side chains modeled explicitly [13] that indicate the desired selectivity of calcium over sodium.

There have been many theoretical studies of K^+ permeation through potassium channels that have made it clear that this is a multi-ion phenomenon involving a 'knock-on' mechanism between ions (see, for example, [1,14–17]). While most of these have discussed the preference for K^+ over Na^+, there has been little discussion of the mechanisms of divalent block and monovalent-divalent ion selectivity.

Here we examine how three types of cation channels discriminate between monovalent and divalent ions. As noted above, voltage-gated potassium and sodium channels allow monovalent ions to pass, but are blocked by divalent ions. In the potassium channel, we examine the competition between Ba^{2+} and K^+. Ba^{2+} can enter the selectivity filter, but binds so strongly to this region that it rarely leaves and so prevents the flow of K^+ ions. Presumably the strong binding is due to electrostatic interaction of the divalent charge with the charge in the channel wall [4]. The specific inhibitory properties of Ba^{2+} have been well analyzed [18–25] and the mean blocking dwell time has been shown to be dependent on the surrounding K^+ concentration. Also, the location at which Ba^{2+} binds in the selectivity filter of the KcsA channel has been determined using X-ray crystallography [4].

As the name suggests, voltage-gated sodium channels readily conduct sodium ions, but the current is affected by divalent ions. Unlike the potassium channel where the presence of divalent ions removes potassium current altogether, in the sodium channel the block by divalent ions is less permanent, and their presence on the internal side of the channel, in particular, acts only to attenuate the sodium current rather than preventing it [5].

In calcium channels, monovalent ions will conduct with no divalent ions present, but these channels also readily conduct divalent calcium ions. Indeed, with a mixture of monovalent and divalent ions present, only the divalent ions will pass through the channel, as the channel selects the divalent ions over the monovalent ones at a ratio of about 1000:1 [3,26].

We demonstrate that the discrimination between ions of different valence as well as all the behavior described above can be understood in terms of the electrostatic interactions between the ions and the channel. The distribution of charges in the channel wall is responsible for the valence selectivity of these channels. After describing the models used in this study, we examine the mechanisms by which each of the channels conducts monovalent ions. We then look at how a solution containing only divalent cations blocks the KcsA potassium and sodium channels but conducts through the calcium channel. Finally, we study the properties of these channels in a mixed solution containing both monovalent and divalent ions.

2. Methods

2.1. Channel models

The channel models we examine here have been studied previously and further details can be found in the original papers: KcsA channel [1], sodium channel [27] and calcium channel [9].

The KcsA channel model is based on the crystal structure determined by Doyle et al. [28]. Because the imaged structure appears to be in a closed state, the intracellular end of the pore must be widened to make a conducting channel [1]. This was done by expanding this section of the channel in molecular dynamics simulations, moving the atoms out of a central 3 Å radius cylindrical region. Once the protein structure has been determined, we create an electrostatic model of the channel by tracing out a pore boundary around the protein atoms as shown in Fig. 1A. The partial charges of the protein atoms are included as point charges, assigned using the CHARMM19 parameter set.

As we do not have a crystal structure of any sodium or calcium channels, we assume a structural similarity of these channels to the family of potassium channels to create models, aided by a variety of experimental results. A model of the family of voltage gated sodium channels was developed by Vora et al. [27] and is pictured in Fig. 1B. Here, the channel protein is represented as a uniform, rigid, low dielectric medium. Dimensions of the external end of the pore are adapted from molecular models [29,30] and include a short, narrow selectivity filter 4 Å in length and a wider external vestibule. The radius of the selectivity filter is set to 2.2 Å as suggested by the permeability of various organic cations [31]. The conductance properties of the channel are highly sensitive to the channel shape used. For example, if we change the diameter of the intracellular or

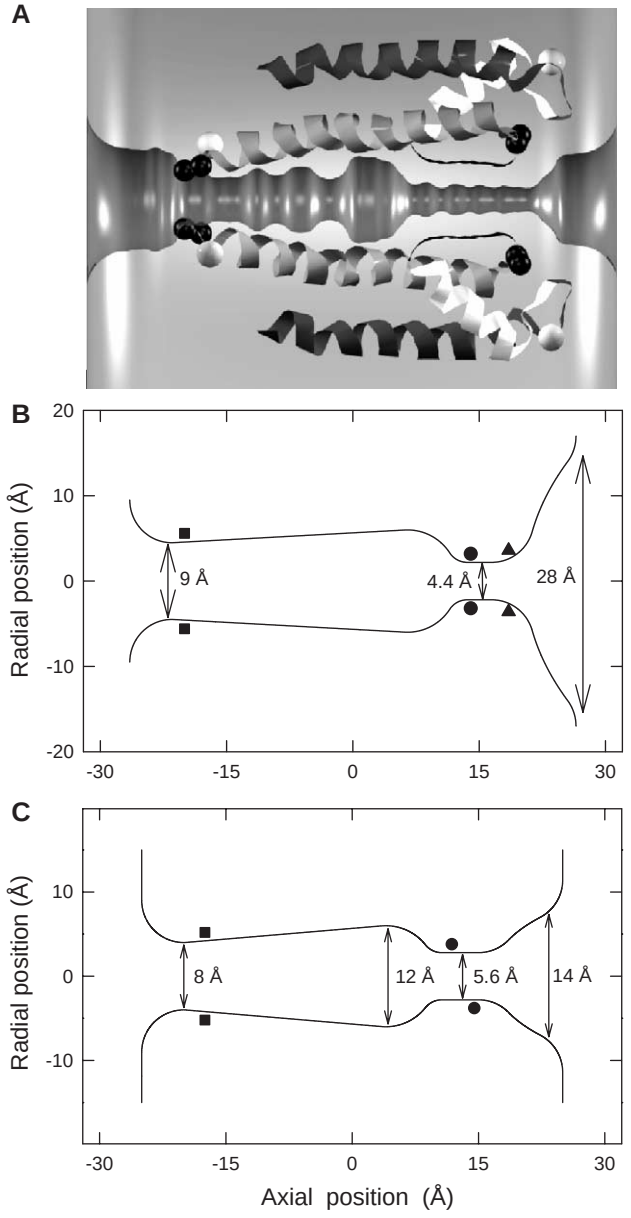

Fig. 1. Channel models. The 3-dimensional channel models are generated by rotating the curves about the central axis by 180°. (A) The KcsA model developed by Chung et al. [1]. Two of the four protein subunits are shown. A dielectric boundary is drawn around the protein atoms as indicated and has a minimum radius of just over 1.4 Å in the selectivity filter. The dark and light spheres represent charged residues. The dark sphere on the right is Asp 80; the dark sphere on the left is Glu 118; the light sphere on the right is Arg 64; and the light sphere on the left side Arg 117. (B) The voltage-gated sodium channel model developed by Vora et al. [27]. The location of the inner and outer rings of charges in the selectivity filter forming P-loops are indicated by the filled circles and triangles. The inner ends of the macroscopic helix dipoles are shown by the squares. (C) Calcium channel model developed by Corry et al. [9]. The positions of two of the four glutamate groups are shown by the circles, and the inner end of 2 of the 4 mouth dipoles by the squares. The other two groups lie into and out of the page. The intracellular end of the channels is on the left and the extracellular side on the right.

extracellular pore entrance or that of the central chamber, the current changes significantly. Indeed the model shown here was found to be the only one with the given broad features that could reproduce all the experimental data.

The calcium channel model developed by Corry et al. [9] again shows a basic similarity to the KcsA pore, with a narrow selectivity filter and a wider central chamber as shown in Fig. 1C. A short external vestibule is included as suggested by molecular models [29,32–34]. The radius of the selectivity filter is determined from the size of the largest permeant cation (tetraethylammonium) as 2.8 Å [35].

Rather than including the partial charges of all the protein atoms in the models of the sodium and calcium channels, we only include a few select charges known to have an important effect on ion conduction. In the sodium channel, two important rings of charged residues lie in the ‘P loops’ that form the selectivity filter and outer vestibule and mutating these has a large effect on the conductance and selectivity of the channel [36–39]. The approximate location of the charged groups can be gauged from the molecular models of these regions [29,30]. An outer ring (at $z=18.5$ Å) contains two aspartate and two glutamate residues. The inner ring (at $z=14$ Å) contains one aspartate, one glutamate and one lysine residue. For our simulation models, we treat these residues as point charges located 1 Å behind the channel protein boundary.

Determining the charge state of these residues in the channel environment is difficult. We expect the lysine residue to remain fully charged, but one or more of the other residues may become protonated. We carried out a systematic study in which we altered the charge of one ring of point charges while holding the total charge of the other constant to find the charge at which the experimental data could be reproduced. As seen in Fig. 2A and B we found that the best agreement with the experimentally determined current of 2.2 pA arose when on average two of the residues were protonated. This additional positive charge was spread across the negative residues such that in the inner ring each acidic residue carried a charge of -1.3×10^{-19} C while in the outer ring each had a charge of -0.95×10^{-19} C. The use of partial charges on the glutamate residues is plausible given that they are known to become protonated in solution as found from the influence of pH on channel currents in sodium [42] and calcium [43–45] channels. Macroscopic helix dipoles are included by analogy with the KcsA structure near the intracellular end of the pore at $z=-20$ Å that aid cations to enter this narrow section of the channel. These dipoles have their negative ends pointing towards the intracellular channel mouth (as shown in Fig. 1B) and represent the carboxyl end of the alpha helices that are believed to lie towards the intracellular side of the channel protein. The positive end of the dipole is located further into the channel protein.

For the calcium channel, mutation experiments have suggested that four glutamate residues line the selectivity filter in close proximity to form a single binding site capable

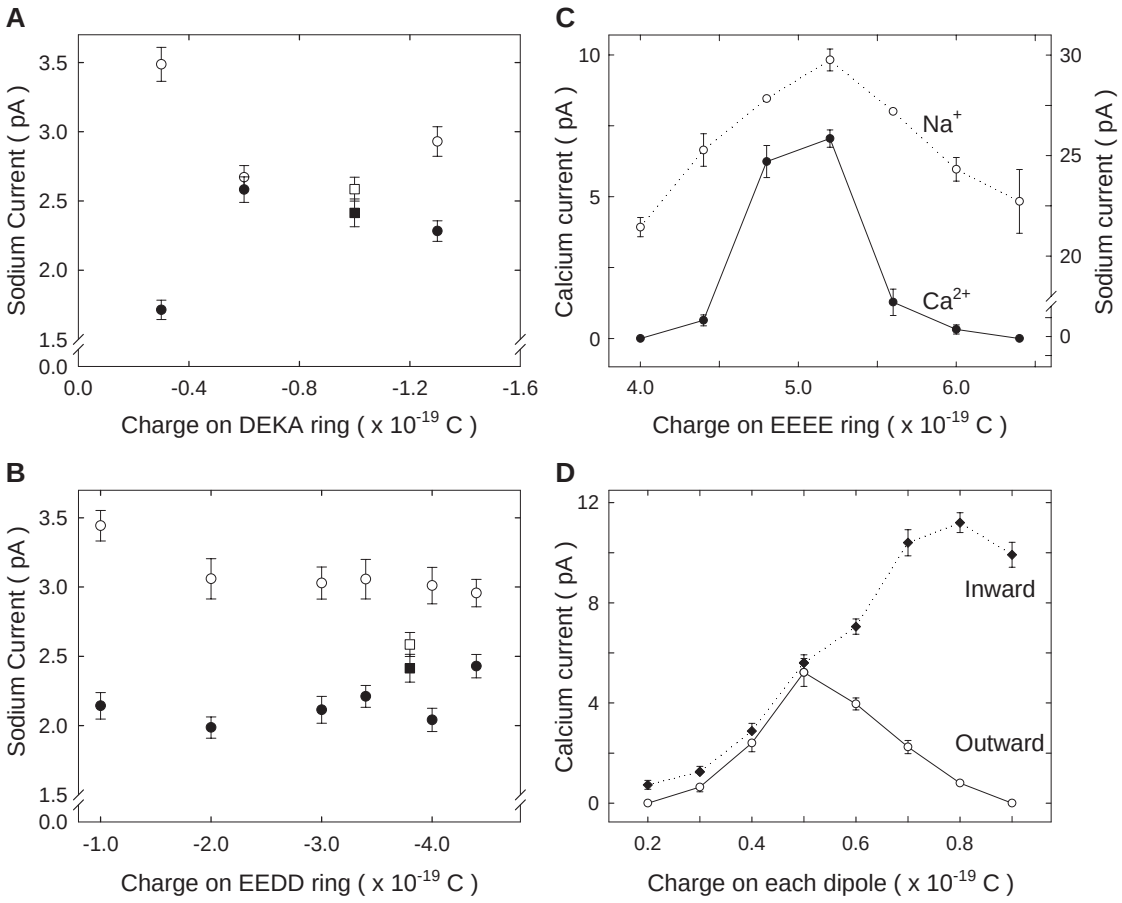

Fig. 2. Effect of fixed charge magnitudes on channel current. (A) Sodium channel. Sodium current obtained while keeping the total charge of the outer ring of EEDD residues fixed at -3.8×10^{-19} C and varying the charge on the DEKA ring. Filled symbols indicate the magnitude of current at an applied potential of +100 mV and open symbols indicate an applied potential of −100 mV. (B) Sodium channel. Sodium current obtained while keeping the total charge of the inner ring of DEKA residues fixed at -1.0×10^{-19} C and varying the charge on the EEDD ring. Symbols as in Panel A. (C) Calcium channel. Sodium (open symbols) and calcium (filled symbols) current obtained with a driving potential of −200 mV for different magnitudes of charge on each glutamate residue in the EEEE locus. (D) Calcium channel. Inward and outward calcium current obtained when the dipole charges varied while the charge on the EEEE residues are held at -1.3×10^{-19} C.

of holding two ions [3,40,41,46], and play a crucial role in determining the permeation characteristics of the channel. These residues are included as point charges in a spiral about the selectivity filter to produce a single, but broad, electrostatic binding site. We conduct a similar study as done for the sodium channel to determine the optimal charge configuration for the EEEE locus, as shown in Fig. 2C. The maximum current of calcium ions through the channel is obtained when each glutamate residue in the ring carries a charge of -1.3×10^{-19} C. Again, macroscopic helix dipoles are included with their negative ends at $z=-17.5$ Å to assist cations entering from the intracellular side of the channel. The charge at each end of the dipole was varied while applying a driving force of −200 mV and it was found that they give an optimal value for inward and outward current when carrying a charge of 0.6×10^{-19} C, as shown in Fig. 2D.

As will be discussed later, for the purposes of this investigation, the exact parameters used to construct the channel models are not important for explaining the selectivity of the channel, although these parameters are crucial for reproducing the experimental conductance values of the channel in all conditions. Provided the selectivity filter is narrow enough to prevent ions from passing each other and the net charge near the filter is roughly correct the important results with respect to selectivity will follow.

2.2. Solution of Poisson's equation

To calculate the electric forces acting on ions in or around the channel, we solve Poisson's equation using a boundary element method [47]. We represent the channel and aqueous solution as continuous dielectric regions. We set this value to $\varepsilon_p=2$ for the protein. On the other hand, the value of the dielectric constant for the aqueous environment inside the channel is less clear. It is likely that in the narrow regions of the channel water molecules will be less able to orient to an electric field than in bulk solution. However, molecular dynamics studies have found

that ions tend to be well solvated in the potassium channel [48]. As it is not known what value is best to use, we use a value of $\varepsilon_w = 60$ in this study as this choice was found to optimise currents in previous simulations of the KcsA channel [1,49].

The potential energy profile encountered by a single ion moving along the pore is obtained by moving an ion along the center of the pore in 1 Å steps and calculating the potential energy at each position. To construct multi-ion energy profiles, we move one of the ions in 1 Å steps, holding it fixed at each step. We then allow the resident ions, placed initially at the binding sites, to adjust their positions so that the force on them will be zero, thus minimizing the total energy of the system. The minimization is performed at each step as we move the test ion and the positions of the ions and the total energy are recorded. Energy minimizations are carried out using a modified version of the steepest descent algorithm [49,50].

2.3. Brownian dynamics simulations

We carry out three-dimensional Brownian dynamics simulations to deduce the conductance properties of the channels and examine the behavior of ions in the channel. In these, we trace the motion of individual ions, but treat the water and protein atoms as a continuous dielectric environment so that we can run simulations for long enough to examine the conductance characteristics of the channel. We place a number of ions in cylindrical reservoirs of radius 30 Å at each end of the channel that mimic the extracellular or intracellular space. The height of the cylinder is adjusted to bring the solution to the desired concentration (usually 150 mM). We then trace the motion of these ions under the influence of electric and random forces using the Langevin equation:

$$m_i \frac{dv_i}{dt} = -m_i \gamma_i v_i + F_i^R + q_i E_i + F_i^S. \quad (1)$$

Here, m_i, v_i, m_i γ_i and q_i are the mass, velocity, friction coefficient and charge on an ion with index i, while F_i^R, E_i and F_i^S are the random stochastic force, systematic electric field, and short range forces experienced by the ion, respectively. We calculate the total force acting on each and every ion in the assembly and then calculate new positions for the ions a short time later. A multiple time-step algorithm is used, where a time-step of $\Delta t = 100$ fs is employed in the reservoirs and 2 fs in the channel where the forces change more rapidly.

Since calculating the electric forces at every step in the simulation is very time consuming, we store pre-calculated electric fields and potentials due to one and two ion configurations in a system of lookup tables [69]. To do this, the electric potential is divided into four components

$$\phi_i = \phi_{X,i} + \phi_{S,i} + \sum_{j \neq i} \left(\phi_{I,ij} + \phi_{C,ij} \right), \quad (2)$$

where the sum runs over all the ions in the system. The symbols in Eq. (2) assume the following significance: $\phi_{X,i}$ is the external potential due to the applied field which stretches from the top of the external reservoir to the bottom of the internal reservoir, fixed charges in the protein wall, and charges induced by these; $\phi_{S,i}$ is the self-potential due to the surface charges induced by the ion i on the channel boundary; $\phi_{I,ij}$ is the image potential felt by ion i due to the charges induced by ion j; and $\phi_{C,ij}$ is the direct interaction between ions i and j. The first three potential terms in Eq. (2) are calculated using a boundary element solution of Poisson's equation as described above. The first term is stored in a three dimensional table while the second and third terms are stored in 2- and 5-dimensional tables utilizing the symmetry developed in the construction of the pore. The ion–ion interactions include the Coulomb term and an oscillating short range potential derived from molecular dynamics simulations as described previously [9], and are calculated on the fly during the simulation. The differences from the traditional Coulomb interaction between ions encountered if the region between the ions spans a dielectric boundary are incorporated in the surface and image charge terms. The short-range forces include these short range ion–ion interactions as well as those between ions and the channel walls.

The Langevin equation is solved with the algorithm of van Gunsteren and Berendsen [51], using the techniques described by Li et al. [52]. The diffusion coefficients of the ions are reduced inside the channel. In the KcsA channel diffusion coefficients are reduced to 50% of their bulk value in the channel. In the sodium channel, the values are reduced to 10% in the selectivity filter and 30% in the remainder of the channel for the sodium ions and 15% and 40% respectively for calcium ions. In the calcium channel, the reductions are to 10% and 50% for calcium ions and 40% and 50% for sodium ions. The exact choice of diffusion coefficient has been shown to only have a small influence on the current passing through the channel [49] but were chosen to agree with molecular dynamics studies [53]. Although molecular dynamics have not been carried out in either the sodium or calcium channels due to the lack of structural information, values of the diffusion constants could be chosen from studies of various ion types in schematic charged and uncharged channels of varying radii. Simulations under various conditions are performed with symmetric ionic concentrations in the two reservoirs. The current is computed from the number of ions that pass through the channel during a simulation period. For further technical details of the Brownian dynamics simulation method, see Chung et al. ([1,49,54]). A stochastic boundary is employed to keep the number of ions in each reservoir constant during the simulation. For example, when an ion passes through the channel the ion furthest from the channel on the side it has passed to is transplanted to a random position in the back portion of the other reservoir. It has been shown previously that this technique yields the same results as if a more complex

Monte-Carlo scheme is used to maintain ion concentrations in the reservoirs [55]. The membrane potential is achieved by applying a uniform field to the system and is incorporated into the solution of Poisson's equation. It should be noted that the resulting potential is far from being linear across the system, but rather drops much more rapidly in the channel than in the reservoirs. Indeed it has been shown that provided the reservoirs are large enough, the potential inside the channel is the same using this approach as when the potential is simply held constant at the boundaries of the system [55].

3. Results and discussion

3.1. Monovalent ions

We first examine how the KcsA, sodium and calcium channels conduct monovalent ions in the absence of any divalent ions. In Fig. 3A, we plot the energy profile seen by a single monovalent ion moving through the KcsA channel (K^+ ion, solid line), sodium channel (Na^+ ion, dotted line) and calcium channel (Na^+ ion, dashed line) with no applied potential. In all cases, the ion experiences a deep energy well created by the negative charges in the channel wall that attract the ion into the selectivity filter region of the channel. The depth of the well is greatest in the potassium channel (60 kT), and least for the sodium channel (20 kT).

These channels will all hold either two (sodium and calcium channels), or three (KcsA channel) monovalent ions in stable equilibrium, and this is only disrupted when another ion enters the channel. When the third ion (or fourth ion in the case of KcsA) enters the channel from the extracellular solution (right side) the energy experienced by the inner most ion if it is to move out of the left side of the channel under an applied potential of −100 mV is plotted in Fig. 3B. Note that in this figure, as well as Figs. 6B and 9, the curves have been aligned vertically for ease of reading so that the base of the energy well in the selectivity filter, rather than the reservoir, is at zero energy. In all cases, the ion sees a small energy barrier, however it can be expected to overcome this during its random thermal motions, especially when it is also aided by the Coulomb repulsion of other cations inside the channel. The energy barrier experienced by this ion is about 4.1 kT high in the KcsA channel, 4.8 kT in the sodium channel, and only 2.5 kT in the calcium channel. From this, we can expect monovalent ions to pass through all of these channels and permeation to involve four ions in KcsA and only three ions in the sodium and calcium channels. Furthermore, we would expect the monovalent current to be highest in the calcium channel, and lowest in the sodium channel, which, as we will discuss below, is in agreement with the experiment.

When we carry out Brownian dynamics simulations we find that, as expected, monovalent ions conduct readily through each of these channel models. In Fig. 4 we plot the current–voltage curves for each channel. For KcsA, the

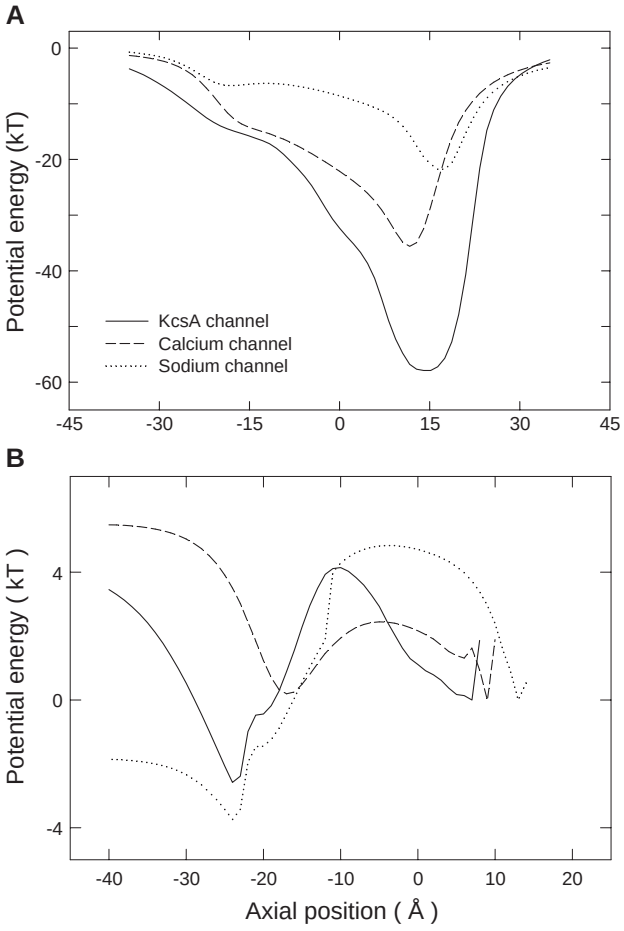

Fig. 3. Energy profiles experienced by monovalent ions. (A) Energy seen by a single monovalent ion moving through the KcsA (solid line), sodium (dotted line) and calcium (dashed line) channels is plotted as it is moved along the channel axis with no applied potential. (B) Multi-ion profiles. The energy of one ion is plotted as it is moved from the selectivity filter to the intracellular vestibule while two other monovalent ions are resident in the binding sites in the selectivity filter under an applied potential of −100 mV driving cations from outside to inside the cell.

current–voltage curve constructed in symmetric 300 mM KCl is not quite linear, rising faster as the applied potential is increased. The mean conductance at 150 mV is around 34 ± 4 pS. Single channel conductance measurements in KcsA channels reveal conductances of 135 pS at 200 mM KCl [56], 97 pS at 250 mM KCl [57] and 83 pS with 100 mM KCl [24]. The conductance found from our simulations is below these values, but Chung et al. [1] have shown that higher conductances can be obtained with this model by slightly widening the intracellular gate of the channel as can be done using a cylindrical repulsive force in molecular dynamics simulations. It should be noted that the selectivity filter, that is responsible for ion selectivity, is not widened in this way, and so the volume of that region remains unchanged in the more highly conductive model.

For the sodium channel, we obtain a linear current–voltage curve of around 24.5 pS slope conductance, as shown in Fig. 4B. The currents obtained agree well with the

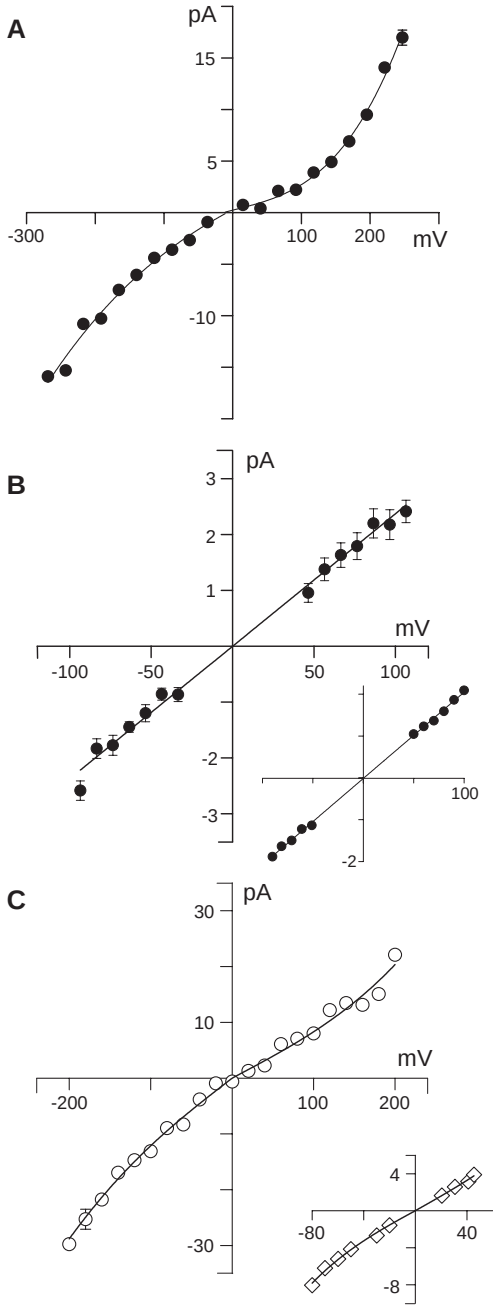

Fig. 4. Current–voltage curves for monovalent ions as found for (A) the KcsA channel with 300 mM KCl, (B) sodium channel with 200 mM NaCl and (C) the calcium channel with 150 mM NaCl. Experimental data under similar conditions is shown in the insets for the sodium [66] and calcium channels [60]. Each data point represents 3, 13 or 0.5 μs of simulation for the KcsA, sodium and calcium channel data respectively. Error bars have length of one standard error of mean.

experimental values of Schild et al. [58] (21 pS) that are reproduced in the inset.

Sodium ions also conduct rapidly through the calcium channel. The current–voltage curve found with 150 mM NaCl in the absence of any divalent ions is shown in Fig. 4C. The conductance is large at 122 pS, much higher than conductances seen for either the potassium or sodium channel as predicted from the energy profile. This high conductance agrees well with that of 85–90 pS found in 150–200 mM solutions [59–61]. The experimental current–voltage curve of Rosenberg and Chen [60] is reproduced in the inset for comparison. At first glance, the fact that the calcium channel conducts sodium ions so well is somewhat surprising given that it is designed to conduct calcium ions, not sodium. However, as we will shortly see, when divalent ions are present, the calcium channel is highly selective allowing only divalent ions to pass.

In Fig. 5, we plot schematically the steps involved in inward monovalent ion permeation in each of the channel models. Under an applied potential, the KcsA channel (Fig. 5A) is normally occupied by 3 or 4 ions. For the sodium and calcium channels, there are always at least two sodium ions in the channel. Conduction involves two main steps, waiting for a third ion to enter the channel (a process that takes 13 ns, 20 ns and 10.5 ns on average for the KcsA, sodium and calcium channels under −100 mV, respectively), and waiting for one of the resident ions to then cross the center of the channel (35 ns, 46 ns and 2.5 ns). The basic steps involved in monovalent ion permeation are the same in all of these channel families and involve the well described ‘knock on’ mechanism.

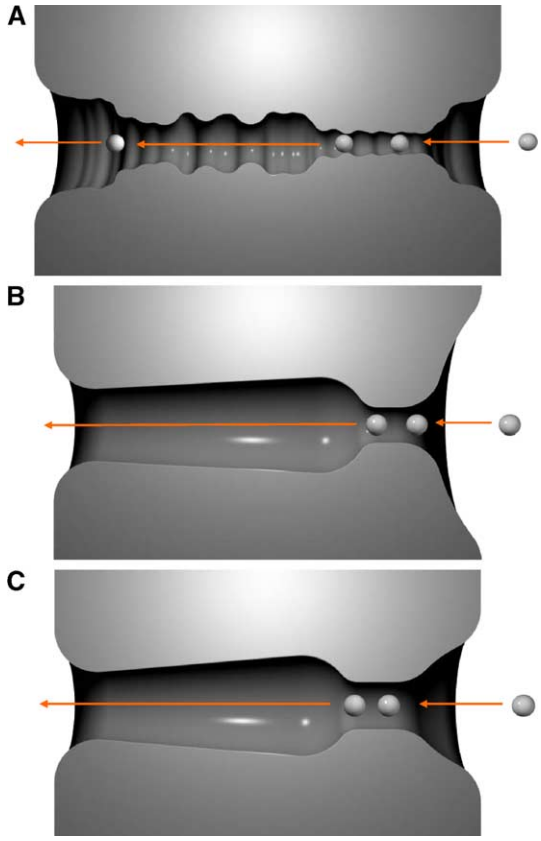

Fig. 5. Schematic diagram of monovalent ion permeation in the KcsA (A), sodium (B) and calcium (C) channels. The most likely location of ions within the channel are indicated and the steps involved in conduction are shown.

3.2. Divalent ions

Next, we examine whether divalent ions will pass through each of these channels in the absence of monovalent ions. In Fig. 6A we show the energy experienced by a single divalent ion crossing each channel with no applied potential. In all cases, the ion sees a deep energy well attracting it to the charges in the selectivity filter. The well is deeper than that seen by a monovalent ion due to the stronger electrostatic attraction to the fixed charges. The depth of the well is 75 kT in KcsA, 33 kT in the sodium channel and 58 kT in the calcium channel. Obviously these ions cannot exit this deep well on their own, and the only chance of an ion permeating through the channel is if another divalent ion enters the channel and assists in pushing the first ion out with its Coulomb repulsion.

In all cases, the charges in the channel are sufficient to attract a second divalent ion into the channel. That is, a second ion also experiences a small energy well attracting it into the channel when one ion resides in the selectivity filter.

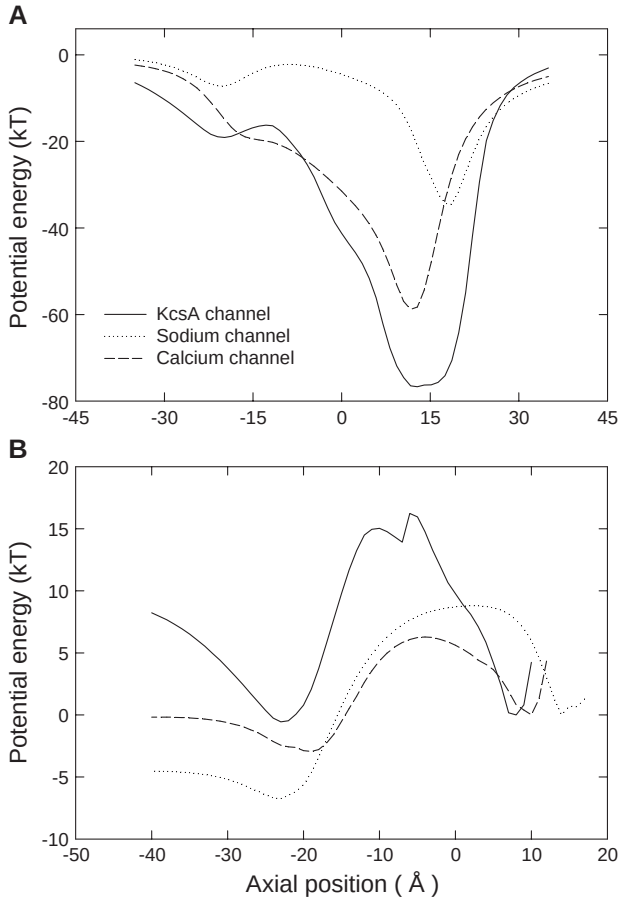

Fig. 6. Energy profiles experienced by divalent ions. (A) Energy seen by a single divalent ion moving through the KcsA (solid line), sodium (dotted line) and calcium (dashed line) channels with no applied potential. (B) Multi-ion profiles, in which the energy of one divalent ion is plotted as it is moved from the selectivity filter to the intracellular vestibule while another divalent ion is resident in the binding site in the selectivity filter under an applied potential of −100 mV.

The energy profile seen by a divalent ion moving from the selectivity filter to the intracellular space when a second divalent ion is in the channel under an applied potential of −100 mV is shown in Fig. 6B. For this first divalent ion to conduct to the intracellular end of the channel, it has to overcome a barrier of almost 17 kT in the KcsA channel, which is extremely unlikely. In the sodium channel, this ion sees an energy barrier of 8.8 kT. Although it is possible for an ion to climb over this with assistance of the Coulomb repulsion of a second ion, we will demonstrate shortly that this is very uncommon. In the calcium channel, however, the energy barrier is lower at only 6.3 kT. Thus, it can be seen that the calcium channel is most likely to conduct divalent ions, while in the other channels, divalent ions may be too strongly bound in the selectivity filter to be able to conduct. It is worth noting that the second calcium ion is attracted closer to the first in the calcium channel than in the sodium channel, and this plays an important role in lowering the energy barrier to Ca^{2+} conduction. Furthermore, as the chance of barrier crossing increases exponentially with barrier height, the 2.5 kT energy difference in the sodium and calcium channels creates a significant difference in currents.

We demonstrate that the calcium channel is the only one that can conduct divalent ions by performing Brownian dynamics simulations on these channel models. In the KcsA channel, we find that no ions cross the channel in 8 μs, even under an applied potential of −200 mV with a symmetric solution of 150 mM $BaCl_2$. With no applied potential, we find that usually only one barium ion occupies the channel and its most likely location is indicated in Fig. 8A. Even though a second barium ion is attracted into the channel, it is more likely to back track out of the channel than the first ion is to cross to the intracellular space.

A similar phenomenon is seen in the sodium channel, where we conducted simulations with 200 mM $CaCl_2$. No ions were seen to cross the channel in 1.6 μs. At an applied potential of −100 mV, one calcium ion is seen to enter the channel and sits in the selectivity filter for the entire time of the simulation. This is where it sees a large energy well, as shown in Fig. 6A. The most likely location of the ion that occupies the channel is shown in Fig. 8B.

In the calcium channel, however, divalent calcium ions do cross the channel, as expected from the energy profiles. The current–voltage curve found with 150 mM $CaCl_2$ is shown in Fig. 7, although the curve is non-linear it shows good agreement with the experimental data of Rosenberg and Chen [60] shown in the inset. At −120 mV, the simulated data has a conductance of 9.7 pS, close to the experimentally determined values of 8.9 pS. The steps involved in conduction are shown in Fig. 8C. One calcium ion is permanently resident in the channel. Conduction involves two main steps: waiting for a second ion to enter the channel, and waiting while the first ion crosses the channel to the intracellular side after the second ion has entered. Under an applied potential of −200 mV the first step takes 11 ns on average and the second 33 ns.

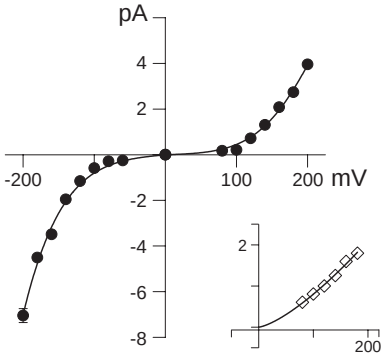

Fig. 7. Current–voltage curve of the calcium channel with symmetric 150 mM $CaCl_2$. Experimental data of Rosenberg and Chen [60] are shown in the inset for comparison. Each data point represents 4 to 8 μs of simulation.

3.3. Mixtures of monovalent and divalent ions

Finally, we examine the case of most interest: mixtures of monovalent and divalent ions. How does each channel select which type of ion to let through and which to stop? As seen previously, the channels are all attractive to both monovalent and divalent ions. Thus, in a mixed solution, the ion that enters the channel first will simply depend on the ion that wanders into the channel entrance first. Therefore, it is important to consider what will happen when both types of ion are resident in the channel.

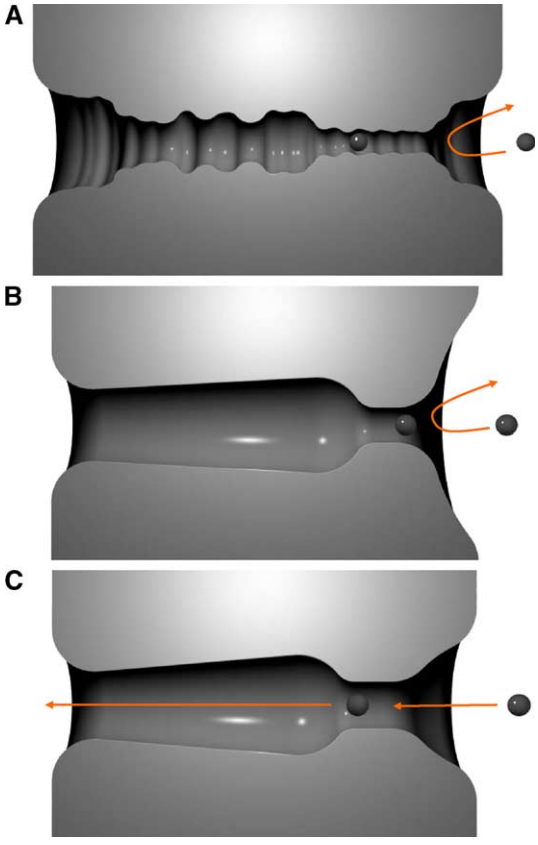

Fig. 8. Schematic diagram of the behavior of divalent ions in the KcsA (A), sodium channel (B) and calcium (C) channels. In the KcsA and sodium channels, one divalent ion resides permanently in the channel. Although a second ion can enter the channel it cannot displace the resident ion and usually backs out of the channel. In the calcium channel, a second ion can displace the resident ion and cause permeation.

The energy to move a resident monovalent ion to the intracellular side of the channel with the aid of another incoming monovalent ion was shown in Fig. 3. In all the channels examined, sodium could be easily displaced allowing sodium to conduct. It is even easier to displace the resident monovalent ion when a divalent ion enters due to larger Coulomb repulsion between the ions. Thus, in all these channels, an incoming divalent ion can displace resident monovalent ions. We have also examined that an incoming divalent ion can displace a resident divalent ion only in the calcium channel. Thus, the only case that remains to be examined is whether an incoming monovalent ion can displace a resident divalent ion.

In the KcsA and sodium channels, the resident divalent ion could not be ejected by another divalent ion. Thus, we should expect that monovalent ions should also not be able to displace it. In Fig. 9, we show that this is indeed the case. In the KcsA channel, the resident divalent ion encounters an energy barrier of 13 kT in the central part of the channel that it must surmount if it is to cross the channel under a −100 mV driving potential. In the sodium channel, the barrier is larger at 15 kT, while it is larger still in the calcium channel. Thus, in all these channels, we cannot expect a monovalent ion to displace a resident divalent ion across the channel.

To examine the conductance properties of the channel in mixed solutions, we again conduct Brownian dynamics simulations. In the KcsA channel, we find that irrespective of whether a K^+ ion enters the selectivity filter first, a Ba^{2+} ion always ends up residing in the selectivity filter of the channel. The Ba^{2+} can enter from either end of the channel (depending on the applied potential) although we find that it enters more easily from the external side of the channel unlike in most experimental results that show that it enters more easily from the internal side [19,24]. Perhaps, a better

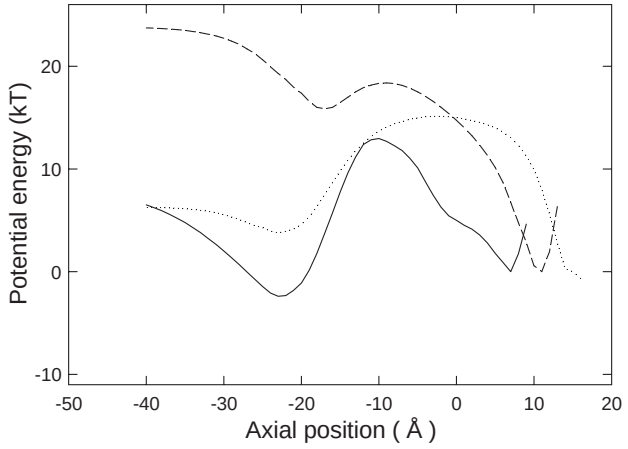

Fig. 9. Multi-ion energy profile in a mixed solution. The energy experienced by a divalent ion as it moves from the selectivity filter to the internal end of the channel is calculated with a monovalent ion present in the selectivity filter under an applied potential of −100 mV. Symbols as in Fig. 3.

agreement with the experiment would be obtained if the pore was widened slightly at the internal end, as suggested previously. It is found experimentally that Ba^{2+} ions do dissociate from their binding site in the channel. Indeed, the block by external Ba^{2+} is relieved over time if Ba^{2+} is removed from the solution [62]. However, the timescale over which this happens is hundreds of milliseconds, well beyond the scope of our simulations.

In Fig. 10, we show where ions dwell within the channel. To construct the plot, we divide the channel into 100 layers and calculate the average number of ions in each layer during a 1.6 μs simulation. Fig. 10A shows the average number of ions in the KcsA channel. On average, there is one Ba^{2+} ion in the channel, but it can inhabit two possible locations, as shown by the two peaks (filled bars) in the figure. There is also usually one K^+ ion in the selectivity filter (and one at the intracellular end of the channel). Depending on the location of the Ba^{2+} ion, the K^+ ion can reside either internal or external to it. If the Ba^{2+} ion resides in the internal site then the K^+ ion stays external to it in what may be the so-called external lock-in site seen in the crystallographic images of Jiang and MacKinnon [4]. The existence of this external lock-in site was also suggested by the fact that the presence of external potassium greatly reduced the dissociation rate of barium to the outside of the cell [21,22]. The barium is much less likely to exit the binding site to the external side of the channel if it is trapped by this external K^+ ion. With the Ba^{2+} ion at the external site, the K^+ ion resides internal to it in what may correspond to the internal lock-in site. Thus, the locations of ions in this channel correspond to those seen in crystallographic data [4].

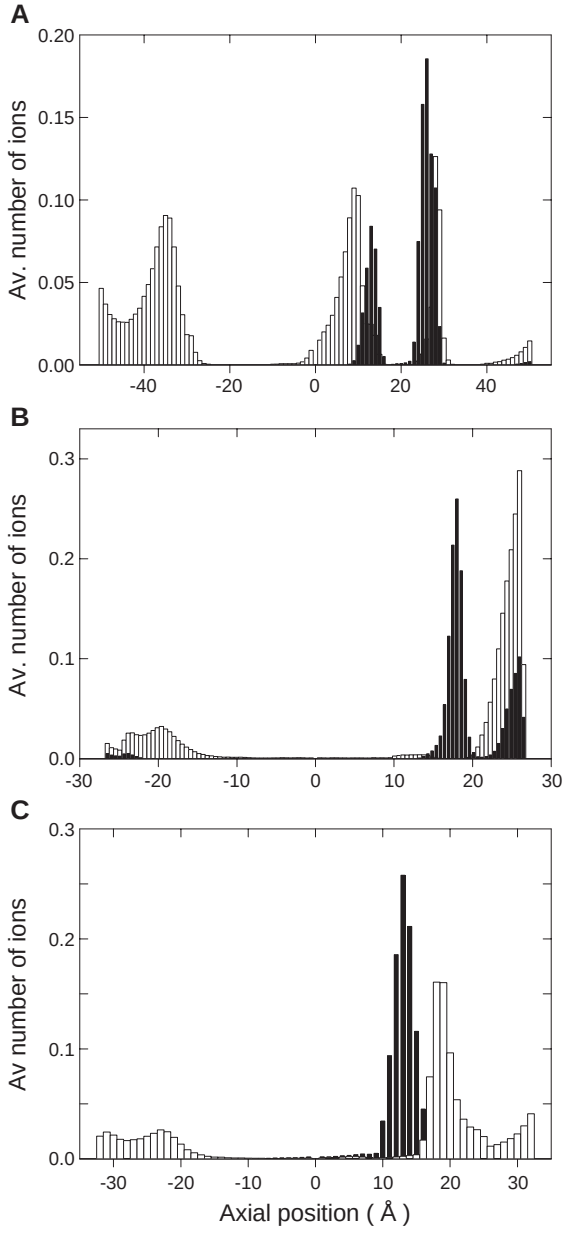

Fig. 10. Dwell histograms in mixed solutions. The average number of monovalent (white bars) and divalent (black bars) ions in layers of the (A) KcsA channel with 300 mM KCl and 150 mM $BaCl_2$ in the reservoirs, (B) sodium channel with 200 mM NaCl and 110 mM $CaCl_2$ in the reservoirs and (C) calcium channel with 150 mM NaCl and 150 mM $CaCl_2$ in the reservoirs.

In the sodium channel, a divalent calcium ion also inevitably ends up residing in the selectivity filter of the channel. The location of the ion is again shown by the dark bars in Fig. 10B. In this case, it can be seen that no monovalent ions reside internal to the divalent ion blocking the channel. It can also be seen that both calcium and sodium ions wander in and out of the external vestibule of the channel, but neither can displace the resident ion or push it across the center of the channel.

The dwell histogram of the calcium channel (Fig. 10C) looks similar to that of the sodium channel. Again, a calcium ion takes up residence in the channel, and sodium ions are seen to enter the external vestibule of the channel. However, the very small number of ions across the center of the channel represents the case of a calcium ion conducting. This, of course, does not arise when a sodium ion enters the external vestibule, but only when a second divalent ion enters.

Next, we show schematically what occurs when ions try to conduct across each channel from outside the cell to inside. In the KcsA channel, a barium ion takes up residence in the channel and although a potassium usually enters, it cannot remove the resident ion and so either remains inside the channel or eventually backs out of the channel (Fig. 11A). In the sodium channel, the divalent calcium ion resides in the channel (pushing a sodium ion out of the way if need be). Sodium or additional calcium ions enter the external vestibule of the channel but cannot displace the resident ion and so usually back out of the channel (Fig. 11B). The calcium channel is similar except that although a sodium ion will back out of the channel, a calcium ion can stay in the selectivity filter and eventually push the resident ion through the channel, as illustrated schematically in Fig. 11C.

Finally, we show current–voltage curves in the presence of mixed monovalent and divalent ion solutions. For the potassium channel, the presence of barium ions almost

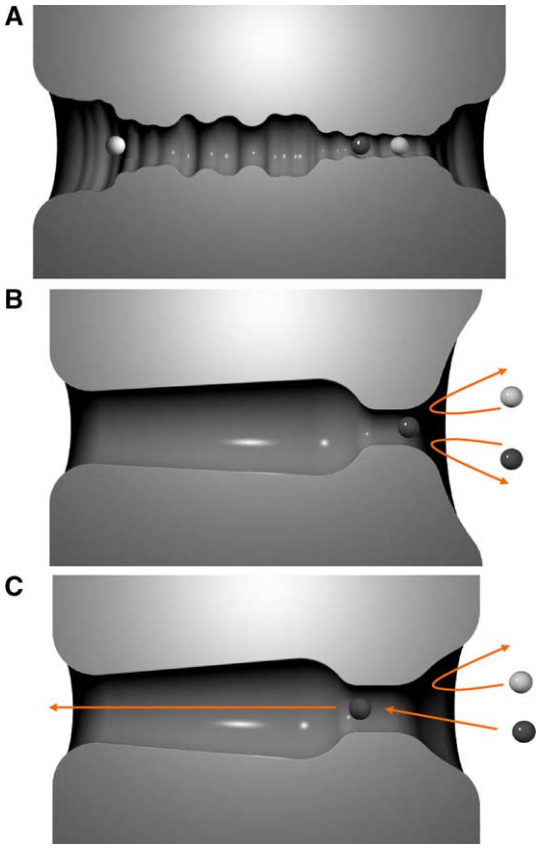

Fig. 11. Schematic diagram showing the behavior of a mixed solution of monovalent (light coloured balls) and divalent (dark coloured balls) cations in the channels. (A) In the KcsA channel, a divalent ion resides in the selectivity filter in conjunction with a monovalent ion. These ions rarely leave the channel. (B) In the sodium channel, a divalent ion again resides in the channel and both monovalent and divalent ions wander in and out of the external vestibule, but neither can displace a resident divalent ion. (C) In the calcium channel a divalent ion will eject any monovalent ions to reside in the EEEE locus of the channel. An incoming monovalent ion cannot displace it and wanders in and out of the external vestibule. If a second divalent ion enters the external vestibule of the channel, it can displace the resident ion and allow conduction.

completely blocks any current. Thus, we do not show a current–voltage curve here. For the sodium channel, the effect of calcium ions on the sodium current is different depending on the direction of conduction as shown in Fig. 12. When ions attempt to move from outside the cell to inside, i.e., under a negative applied potential, divalent ions can easily enter the selectivity filter and block the sodium current. Thus, this side of the current–voltage curve (filled circles) shows almost no current, a dramatic difference from the results seen without calcium ions present (open circles). However, when ions are moving from inside the cell to outside, the picture is quite different. There are almost always two sodium ions sitting in the selectivity filter which have entered the channel from the extracellular side. Intracellular calcium ions see a large energy barrier in the central part of the channel and do not move into the selectivity filter. This barrier is generated by the image forces the calcium ion experiences in the narrow inner chamber, as well as from the repulsive force of the sodium ions sitting in their equilibrium positions in the selectivity filter. The calcium ions do, however, attenuate the sodium current by temporarily occupying the shallow energy well at the internal end of the channel ($z \approx -20$ Å). The well is not deep enough to permanently hold the ions and they only dwell there temporarily before exiting back into the internal solution, however whilst they are there they prevent sodium permeation and thus attenuate the current. For the calcium channel, the presence of sodium ions slightly attenuates the conduction of calcium ions in a similar manner. When a calcium ion is resident in the channel, the sodium ions will not permeate through but they can get in the way of a second calcium ion entering as is required for calcium conduction. The attenuation of calcium currents by sodium seen in our model has been shown previously to be in excellent agreement with experimental data [9] and is not reproduced here.

The case of the calcium channel is perhaps the most interesting. We have seen that it will conduct sodium ions in the absence of calcium. So how does it select out the calcium ions in a mixed solution? The answer can be seen to rely on the perfect balance of how strongly a calcium ion is bound in the channel. If a calcium ion is resident in the channel, it will only leave with the aid of Coulomb repulsion from another ion entering the channel. If the calcium ion is bound too strongly or if a second ion cannot approach close enough to it, then as was seen for the potassium and sodium channels, it would not be displaced by any incoming ion. If the calcium ion is only weakly bound then it will be displaced by either a sodium or calcium ion and both will conduct. However, if it lies between these extremes then it is possible that the resident calcium ion will only be displaced by an incoming calcium ion and not a sodium ion. The reason, of course, is that a sodium ion carries only a monovalent charge while a calcium ion is divalent. Thus, there is a much greater

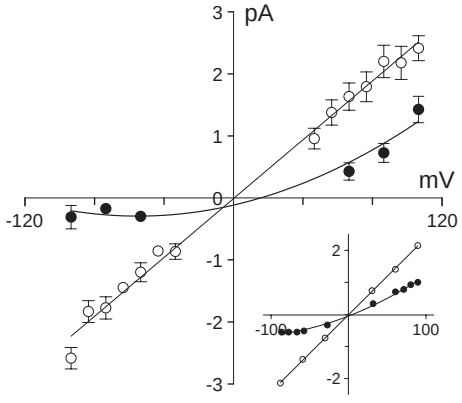

Fig. 12. Current–voltage curve of the sodium channel in a mixed symmetrical solution of 200 mM NaCl and 110 mM $CaCl_2$. Data for the mixed solution (filled circles) is compared to the current–voltage curve obtained with only 200 mM NaCl solution (open circles). The experimental data of French et al. [5] in similar conditions is shown in the inset for comparison. Data points represent 6.4 μs of simulation.

Coulomb repulsion between two calcium ions than between a calcium and a sodium ion.

This balance can be seen in the energy profiles shown in Fig. 9. If a calcium ion is resident in the channel, then the energy barrier it must overcome to cross to the internal end of the channel when a sodium ion enters from the external side (from the right) is shown by the dashed line in Fig. 9. Even with the aid of the Coulomb repulsion of the sodium ion, the calcium ion has a barrier of over 18 kT. The calcium ion cannot be expected to overcome this barrier, and so the ion will not be displaced by a sodium ion. Indeed, even if two sodium ions were to enter together, they would not be able to displace the calcium ion [9]. However, as seen in Fig. 6B, a calcium ion only sees a barrier of 6.3 kT when another calcium ion enters the channel. Thus, only an incoming calcium ion can displace an ion from the channel and enable conduction.

Notably, our calcium channel model explains the five important experimental observations highlighted by Sather and McCleskey [3]. The channel gains its high selectivity by strongly binding calcium ions such that they cannot be displaced by sodium. By utilizing ion–ion repulsion in the multi ion channel, the current passing through the channel is still large. The broad electrostatic binding region of the EEEE locus can hold two calcium ions or three sodium ions at any time. Calcium blocks the channel with high apparent affinity due to its strong electrostatic attraction to the glutamate residues, but it can leave the channel at a lower apparent affinity due to the aid of ion–ion repulsion. Finally, it is the electrostatic attraction of the glutamate residues that forms a high affinity electrostatic binding site. We point out the criticism raised by Sather and McCleskey [3] about this model, that the short range ion–ion interactions have undefined origin, is not correct. The ion–ion interactions in our models simply include the Coulomb interaction, short range repulsion to mimic the overlap of electron clouds, and a damped oscillating potential. The oscillating potential is created by the presence of water molecules, i.e., ions prefer to be separated by an integer number of molecules than somewhere in between and is well described by molecular dynamics simulations [67,68].

In addition to these observations, our calcium channel model can also replicate a large range of physiological data. Not only does the model reproduce the conductance of the channel for sodium and calcium ions it also replicates more complex properties found in mixtures of ions. Firstly, as calcium ions are added to NaCl solution on each side of the channel, the channel current is seen to first fall and then increase again as the calcium concentration is increased [63]. This so-called ‘anomalous mole fraction effect’ is reproduced in our model [9] and is a direct consequence of the selectivity of the channel. With no calcium present, sodium flows through the channel. As the calcium concentration is increased, sodium will have a window in which it can conduct before a calcium ion finds its way into the selectivity filter of the channel, but the net current falls. At high calcium concentrations, calcium enters the filter quickly, thus rapidly stopping sodium current. However, at such concentrations, the chance of a second calcium entering the channel increases and so calcium current begins to flow through the channel. However, the current carried by calcium at high calcium concentration is somewhat attenuated by the presence of sodium in accord with experiment [9,64] as the sodium effectively gets in the way of the second calcium ion. By ‘hanging around’ in the external vestibule of the channel, it temporarily prevents the second calcium ion from entering the selectivity filter and slows conduction.

One might ask why the calcium channel holds only three sodium ions in the selectivity filter rather than four, given that there are four glutamate residues, and the filter and holds two calcium ions. Because the glutamate residues are not fully charged, charge neutrality is best achieved with either two calcium ions or three sodium ions. Furthermore, it can be seen from Fig. 2C that if the residues were fully charged, the channel would stop passing calcium ions, while still conducting monovalent ions in a pure solution, and most likely be blocked by divalent ions in a mixed solution.

The KcsA channel, in contrast, does not show an anomalous mole fraction behavior between K^+ and Ba^{2+} ions. In a mixed solution, K^+ will again have a chance to permeate through the channel before Ba^{2+} enters and blocks the channel. However, the K^+ current rapidly drops as the Ba^{2+} concentration increases. The current does not get higher at large Ba^{2+} concentrations, as in the calcium channel, because Ba^{2+} does not conduct, even when a second Ba^{2+} ion enters the channel.

Table 1
Summary of results and comparison to experimental data

Condition	KcsA channel		Na channel		Ca channel	
	Sim	Exp	Sim	Exp	Sim	Exp
Barrier to monovalent permeation (kT)	4.1		4.8		2.5	
Barrier to divalent permeation (kT)	17		8.8		6.3	
Monovalent conductance (pS)	34 (150 mM)	83 (100 mM)	25 (150 mM)	21 (150 mM)	122 (150 mM)	90 (150 mM)
Divalent conductance (pS)	0	0	0	0	9.7 (150 mM)	9.0 (150 mM)
Result in mixed solution	No current	No current	Large asymmetric attenuation	Large asymmetric attenuation	Small attenuation	Small attenuation

Results are shown for simulations (Sim) with monovalent ions (K^+ for KcsA, Na^+ for Na and Ca channel), divalent ions (Ba^+ for KcsA, Ca^+ for Na and Ca channels), and mixtures of these, and compared to experimental data (Exp).

A summary of some of the main results and a comparison with experimental data is shown in Table 1.

4. Concluding remarks

Although the model of the KcsA channel is based on a crystal structure, those of the sodium and calcium channel are only hypotheses that assume structural similarity to the KcsA channel. However, we gain confidence in these models by their ability to reproduce and explain a wealth of experimental data including current–voltage and current–concentration curves, the inhibition of calcium currents by sodium ions in the calcium channel and of sodium currents by internal calcium in the sodium channel, the anomalous mole fraction behavior between monovalent and divalent ions and the mutation of key residues [1,9,27]. The KcsA, sodium, and calcium channel models presented here reproduce all experimentally measured properties in the presence of monovalent ions, divalent ions and mixed solutions. Monovalent ions are seen to pass through all of these channels using a 'knock on' mechanism. Divalent ions bind more strongly in the selectivity filter due to the stronger electrostatic attraction to the negative charges in the protein. The different attraction of monovalent and divalent ions to the channel protein is responsible for the valence discrimination of our channel models.

As noted in the Introduction, an alternative theory has been proposed by Boda et al. [11,65] and Nonner et al. [10] to explain the selectivity mechanisms of the calcium and sodium channels. They propose that it is a charge versus volume competition mechanism that works in the calcium channel to select calcium over sodium ions. Although this model and ours share a similarity in that the electrostatic attraction between the glutamate oxygens and permeating ions are the cause of valence selectivity, the mechanism is significantly different. In our case, volume is only important in that the selectivity filter is narrow enough such that ions may not pass each other in the channel. Beyond that, volume does not play a role. Ca^{2+} ions are not favored over Na^{+} because they occupy less volume. Rather, they are preferred because they are attracted more strongly to the selectivity filter than Na^{+}. We notice that due to their divalent charge, calcium ions see a much larger energy well in the selectivity filter than monovalent ions. Therefore, even if there are two sodium ions sitting in the filter region, a calcium ion is able to push these ions out of the channel and replace them in the selectivity filter. On the other hand, once a calcium ion is inside the selectivity filter, only other calcium ions, due to a larger repulsion from its divalent charge, are able to continue the process of conduction by pushing the resident ion out of the channel. In our model, there is ample volume for ions in the selectivity filter. Furthermore, the mechanism of selectivity is not critically dependent on the structure and available volume for ions in the selectivity filter as it may be in the alternative model. Indeed, changing the volume of the filter need not alter our selectivity results, as although the conductance of the channel is sensitive to this parameter, the selectivity of the channel is not (provided ions cannot pass each other in the filter).

The stochastic model described here cannot discriminate between ions of the same valence. Thus, we cannot describe why Ba^{2+}, for example, conducts through calcium channels at a greater rate than Ca^{2+} or why it is blocked by Zn^{2+}. Such phenomena are probably a result of the detailed interaction between these ions, the protein atoms and surrounding molecules and are more likely to be elucidated using classical or ab initio molecular dynamics studies or by including ion-specific desolvation barriers into our simulations.

Irrespective of the accuracy of the models used, these results prove a more general point: that the selectivity of cation channels to ions of different valence can be explained in terms of electrostatic properties. That monovalent ions conduct through all these channels but that divalent ions block the KcsA and sodium channels and conduct through calcium channels is a consequence of the interaction between the charges on the ions, partial charges on the protein and repulsion induced on the dielectric walls of the channel. The same results would be possible if the shape of the models is altered, provided the channel remains narrow enough that ions cannot pass each other and that the strength of the charges creates the same binding effects seen here. Indeed, the selectivity of the channels could be reproduced in simple cylindrical models surrounded by appropriate charges (however, it seems unlikely that such a model could reproduce all the physiological data). Nor do these models rely on having a fixed protein. The protein does not change shape as an ion permeates through in these models, as this is the simplest way in which to conduct our simulations. This fixed structure is meant to represent the average coordinates of the protein atoms. However, the electrostatic basis of valence selectivity could also be in effect if, for example, the glutamate side chains in the EEEE locus, are more free to move as in the models of Boda et al. [11], Nonner et al. [10], Yang and Henderson [12] or Ramakrishnan et al. [13]. It is the electrostatic effect of the charges on these atoms that is important to gain the valence discrimination seen here, not their mobility. Thus, the valence selectivity of these channels appears to be a consequence of the electrostatic interaction of the ions with the distribution of partial charges in the protein and need not rely on the volume of the channel or any more complex effects.

References

[1] S.H. Chung, T.W. Allen, S. Kuyucak, Conducting-state properties of the KcsA potassium channel from molecular and Brownian dynamics simulations, Biophys. J. 82 (2002) 628–645.

[2] S. Edwards, B. Corry, S. Kuyucak, S.H. Chung, Continuum electrostatics fails to describe ion permeation in the gramicidin channel, Biophys. J. 83 (2002) 1348–1360.
[3] W.A. Sather, E.W. McCleskey, Permeation and selectivity in calcium channels, Annu. Rev. Physiol. 65 (2003) 133–159.
[4] Y. Jiang, R. MacKinnon, The barium site in a potassium channel by X-ray crystallography, J. Gen. Physiol. 115 (2000) 269–272.
[5] R.J. French, J.F. Worley III, W.F. Wonderlin, A.S. Kularatna, B.K. Krueger, Ion permeation, divalent ion block and chemical modification of single sodium channels, J. Gen. Physiol. 103 (1994) 447–470.
[6] P. Hess, R.W. Tsien, Mechanism of ion permeation through calcium channels, Nature 309 (1984) 453–456.
[7] W. Almers, E.W. McCleskey, Non-selective conductance in calcium channels of frog muscle: calcium selectivity in a single file pore, J. Physiol. 353 (1984) 585–608.
[8] B. Corry, T.W. Allen, S. Kuyucak, S.H. Chung, A model of calcium channels, Biochim. Biophys. Acta 1509 (2000) 1–6.
[9] B. Corry, T.W. Allen, S. Kuyucak, S.H. Chung, Mechanisms of permeation and selectivity in calcium channels, Biophys. J. 80 (2001) 195–214.
[10] W. Nonner, L. Catacuzzeno, B. Eisenberg, Binding and selectivity in L-type Ca channels: a mean spherical approximation, Biophys. J. 79 (2000) 1976–1992.
[11] D. Boda, D. Busath, D. Henderson, S. Sokolowski, Monte Carlo simulations of the mechanism for channel selectivity: the competition between volume exclusion and charge neutrality, J. Phys. Chem. 104 (2000) 8903–8910.
[12] Y. Yang, D. Henderson, D. Busath, Applied-field molecular dynamics study of a model calcium channel selectivity filter, J. Chem. Phys. 118 (2003) 4213–4220.
[13] V. Ramakrishnan, D. Henderson, D.D. Busath, Applied field non-equilibrium molecular dynamics simulations of ion exit from a β-barrel model of the L-type calcium channel, Biochim. Biophys. Acta 1664 (2004) 1–8.
[14] S. Berneche, B. Roux, A microscopic view of ion conduction through the K^+ channel, Proc. Natl. Acad. Sci. 100 (2003) 8644–8648.
[15] J. Åqvist, V. Luzhkov, Ion permeation mechanism of the potassium channel, Nature 404 (2000) 881–884.
[16] A. Burykin, M. Kato, A. Warshel, Exploring the origin of the selectivity of the KcsA potassium channel, Proteins 52 (2003) 412–416.
[17] C. Domene, M. Sansom, Potassium channel, ions, and water: simulation studies based on the high resolution X-ray structure of KcsA, Biophys. J. 85 (2003) 2787–2800.
[18] D.C. Eaton, M. Brodwick, Effects of barium on the potassium conductance of squid axon, J. Gen. Physiol. 75 (1980) 727–750.
[19] C.M. Armstrong, R.P. Swenson Jr., S.R. Taylor, Block of squid axon K channels by internally and externally applied barium ions, J. Gen. Physiol. 80 (1982) 663–682.
[20] C. Miller, Trapping single ions inside single ion channels, Biophys. J. 52 (1987) 123–126.
[21] J. Neyton, C. Miller, Potassium blocks barium permeation through a calcium-activated potassium channel, J. Gen. Physiol. 92 (1998) 549–567.
[22] J. Neyton, C. Miller, Discrete Ba^{2+} block as a probe of ion occupancy and pore structure in the high-conductance Ca^{2+} activated K^+ channel, J. Gen. Physiol. 92 (1998) 569–586.
[23] C.D. Benham, T.B. Bolton, R.J. Lang, T. Takewaki, The mechanism of action of Ba^{2+} and TEA on single Ca^{2+}-activated K^+-channels in arterial and intestinal smooth muscle cell membranes, Pflugers Arch. 403 (1985) 120–127.
[24] L. Heginbotham, M. LeMasurier, L. Kolnakova-Partensky, C. Miller, Single *Streptomyces lividans* K^+ channels: functional asymmetries and sidedness of proton activation, J. Gen. Physiol. 114 (1999) 551–559.
[25] C. Vergara, O. Alvarez, R. Latorre, Localization of the K^+ lock-in and the Ba^{2+} binding sites in a voltage gated calcium modulated channel, J. Gen. Physiol. 114 (1999) 365–376.
[26] P. Hess, Elementary properties of cardiac calcium channels: a brief review, Can. J. Physiol. Pharm. 66 (1987) 1218–1223.
[27] T. Vora, B. Corry, S.H. Chung. A model of sodium channels. Biochim. Biophys. Acta 1668 (2005) 106–116.
[28] D.A. Doyle, J.M. Cabral, R.A. Pfuetzner, A. Kuo, J.M. Gulbis, S.L. Cohen, B.T. Chait, R. MacKinnon, The structure of the potassium channel: molecular basis of K^+ conduction and selectivity, Science 280 (1998) 69–77.
[29] H.R. Guy, S.R. Durell, Structural models of Na^+, Ca^{2+}, and K^+ channels, Soc. Gen. Physiol. Ser. 50 (1995) 1–16.
[30] G.M. Lipkind, H.A. Fozzard, KcsA crystal structure as a framework for a molecular model of the Na^+ channel pore, Biochemistry 39 (2000) 8161–8170.
[31] B. Hille, The permeability of the sodium channel to organic cations, J. Gen. Physiol. 58 (1971) 599–619.
[32] J.A. Schetz, P.A.V. Anderson, A reevaluation of the structure of the pore region of voltage activated cation channels, Biol. Bull. 185 (1993) 462–466.
[33] S.W. Doughty, F.E. Blaney, W.G. Richards, Models of ion pores in N-type voltage gated calcium channels, J. Mol. Graph. 13 (1995) 342–348.
[34] S.W. Doughty, F.E. Blaney, B.S. Orlek, W.G. Richards, A molecular mechanism for toxin block in N-type calcium channels, Protein Eng. 11 (1998) 95–99.
[35] E.W. McCleskey, W. Almers, The Ca channel in skeletal muscle is a large pore, Proc. Natl. Acad. Sci. U. S. A. 82 (1985) 7149–7153.
[36] S.H. Heinemann, H. Terlau, W. Stuhmer, K. Imoto, S. Numa, Calcium channel characteristics conferred on the sodium channel by single mutations, Nature 356 (1992) 441–443.
[37] T. Schlief, R. Schönherr, K. Imoto, S.H. Heinemann, Pore properties of rat brain: II. Sodium channels mutated in the selectivity filter domain, Eur. Biophys. J. 25 (1996) 75–91.
[38] Y.M. Sun, I. Favre, L. Schild, E. Moczydlowski, On the structural basis for size-selective permeation of organic cations through the voltage-gated sodium channel — effect of alanine mutations at the DEKA locus on selectivity, inhibition by Ca^{2+} and H^+, and molecular sieving, J. Gen. Physiol. 110 (1997) 693–715.
[39] W.A. Catterall, From ionic currents to molecular mechanisms: the structure and function of voltage-gated sodium channels, Neuron 26 (2000) 13–25.
[40] J. Yang, P.T. Ellinor, W.A. Sather, J.F. Zhang, R.W. Tsien, Molecular determinants of Ca^{2+} selectivity and ion permeation in L-type Ca^{2+} channels, Nature 366 (1993) 158–161.
[41] P.T. Ellinor, J. Yang, W.A. Sather, J.F. Zhang, R.W. Tsien, Ca^{2+} channel selectivity at a single locus for high-affinity Ca^{2+} interactions, Neuron 15 (1995) 1121–1132.
[42] J.F. Zhang, S.A. Siegelbaum, Effects of external protons on single cardiac sodium channels from guinea pig ventricular myocytes, J. Gen. Physiol. 98 (1991) 1065–1083.
[43] X.H. Chen, I. Bezprozvanny, R.W. Tsien, Molecular basis of proton block of L-type Ca^{2+} channels, J. Gen. Physiol. 108 (5) (1996) 363–374.
[44] M.J. Root, R. MacKinnon, Two identical noninteracting sites for an ion channel revealed by proton transfer, Science 265 (1994) 1852–1856.
[45] X.H. Chen, R.W. Tsien, Aspartate substitutions establish the concerted action of p-region glutamates in repeats I and III in forming the protonation site of L-type Ca^{2+} channels, J. Biol. Chem. 272 (1997) 30002–30008.
[46] A. Bahinski, A. Yatani, G. Mikala, S. Tang, S. Yamamoto, A. Schwartz, Charged amino acids near the pore entrance influence ion-conduction of a human L-type cardiac calcium channel, Mol. Cell. Biochem. 166 (1997) 125–134.
[47] M. Hoyles, S. Kuyucak, S.H. Chung, Energy barrier presented to ions by the vestibule of the biological membrane channel, Biophys. J. 70 (1996) 1628–1642.
[48] T.W. Allen, A. Bliznyuk, A.P. Rendell, S. Kuyucak, S.H. Chung, The

potassium channel: structure, selectivity and diffusion, J. Chem. Phys. 112 (2000) 8191–8204.
[49] S.H. Chung, T.W. Allen, M. Hoyles, S. Kuyucak, Permeation of ions across the potassium channel: Brownian dynamics studies, Biophys. J. 77 (1999) 2517–2533.
[50] W.H. Press, B.P. Flannery, S.A. Teukolsky, W.T. Vetterling, Numerical Recipes, Cambridge University Press, Cambridge, 1989.
[51] W.F. van Gunsteren, H.J.C. Berendsen, Algorithms for Brownian dynamics, Mol. Phys. 45 (1982) 637–647.
[52] S.C. Li, M. Hoyles, S. Kuyucak, S.H. Chung, Brownian dynamics study of ion transport in the vestibule of membrane channels, Biophys. J. 74 (1998) 37–47.
[53] T.W. Allen, S. Kuyucak, S.H. Chung, Molecular dynamics estimates of ion diffusion in model hydrophobic and the KcsA potassium channels, Biophys. Chem. 86 (2000) 1–14.
[54] S.H. Chung, M. Hoyles, T.W. Allen, S. Kuyucak, Study of ionic currents across a model membrane channel using Brownian dynamics, Biophys. J. 75 (1998) 793–809.
[55] B. Corry, M. Hoyles, T.W. Allen, M. Walker, S. Kuyucak, S.H. Chung, Reservoir boundaries in Brownian dynamics simulations of ion channels, Biophys. J. 82 (2002) 1975–1982.
[56] L.G. Ceullo, J.G. Romero, D.M. Cortes, E. Perozo, pH dependent gating in the *Streptomyces lividans* K^+ channel, Biochemistry 37 (1998) 3229–3236.
[57] D. Meuser, H. Splitt, R. Wagner, H. Schrempf, Exploring the open pore of the potassium channel from *Streptomyces lividans*, FEBS Lett. 462 (1999) 447–452.
[58] L. Schild, A. Ravindran, E. Moczydlowski, Zn^{2+}-induced subconductance events in cardiac Na^+ channels prolonged by batrachotoxin. Current–voltage behavior and single-channel kinetics, J. Gen. Physiol. 97 (1991) 117–142.
[59] P. Hess, J.B. Lansman, R.W. Tsien, Calcium channel selectivity for divalent and monovalent cations: voltage and concentration dependence of single channel current in ventricular heart cells, J. Gen. Physiol. 88 (1986) 293–319.
[60] R.L. Rosenberg, X.H. Chen, Characterization and localization of two ion-binding sites within the pore of cardiac L-type calcium channels, J. Gen. Physiol. 97 (1991) 1207–1225.
[61] B. Nilius, P. Hess, J.B. Lansman, R.W. Tsien, A novel type of cardiac calcium channel in ventricular cells, Nature 316 (1985) 443–446.
[62] R.E. Harris, H.P. Larson, E.Y. Isacoff, A permanent ion binding site located between two gates of the shaker K^+ channel, Biophys. J. 74 (1998) 1808–1820.
[63] W. Almers, E.W. McCleskey, P.T. Palade, A non-selective cation conductance in frog muscle membrane blocked by micromolar external calcium ions, J. Physiol. 353 (1984) 565–583.
[64] L. Polo-Parada, S.J. Korn, Block of N-type calcium channels in chick sensory neurons by external sodium, J. Gen. Physiol. 109 (1997) 693–702.
[65] D. Boda, D. Busath, B. Eisenberg, D. Henderson, W. Nonner, Monte Carlo simulations of ion selectivity in a biological Na channel: charge–space competition, Phys. Chem. Chem. Phys. 4 (2002) 5154–5160.
[66] L. Schild, E. Moczydlowski, Permeation of Na^+ through open and Zn^{2+}-occupied conductance states of cardiac sodium channels modified by batrachotoxin: exploring ion–ion interactions in a multi-ion channel, Biophys. J. 66 (1994) 654–666.
[67] E. Guárdia, R. Rey, J.A. Padró, Na^+–Na^+ and Cl^-–Cl^- ion pairs in water: mean force potentials by constrained molecular dynamics, J. Chem. Phys. 95 (1991) 2823–2831.
[68] E. Guárdia, R. Rey, J.A. Padró, Potential of mean force by constrained molecular dynamics: a sodium chloride ion-pair in water, J. Chem. Phys. 155 (1991) 187–195.
[69] M. Hoyles, S. Kuyucak, S.H. Chung, Computer simulation of ion conductance in membrane channels, Phys. Rev. E 58 (1998) 3654–3661.